

# Unsupervised Change Detection in VHR Images Based on Morphological Profiles and Automated Training Sample Extraction

Xin Wang\*, Peijun Du\*, Sicong Liu<sup>†</sup>, Yaping Meng\*, Cong Lin\*

\*School of Geography and Ocean Science, Nanjing University, Nanjing, China

<sup>†</sup>College of Surveying and Geoinformatics, Tongji University, Shanghai, China

Email: wangxrs@126.com, dupjrs@126.com, sicong.liu@tongji.edu.cn, ypmengnju@126.com, lcnjucumt@126.com

**Abstract**—VHR remote sensing image change detection with pixel-based method often results in some problems that have negative effects on accuracy, such as the salt-and-pepper noise. In order to achieve a better result under this circumstance, an unsupervised sequential strategy combining Morphological Profiles and automated training sample extraction is introduced. Change detection with two real multi-temporal VHR datasets were carried out to test the effectiveness of the proposed approach. The experimental results showed that this approach outperformed the traditional unsupervised change detection methods in terms of accuracy and visual effect.

**Index Terms**—Morphological Profiles (MPs), Change Vector Analysis (CVA), Markov Random Field (MRF), automated training sample extraction (ATSE)

## I. INTRODUCTION

Land surface has been significantly modified in recent years due to the increasing human activities [1]. Earth observation through satellite images provides an effective mean for monitoring land cover change and multi-temporal remote sensing image change detection has been widely used in many applications such as agriculture, environment and urban planning [2]. With the development of remote sensing technology, the spatial resolution of remote sensing images is increasing rapidly. Compared to traditional images with medium and low spatial resolutions, the detailed information of ground objects can be more clearly expressed and analyzed in VHR images [3].

From the perspective of processing unit, change detection methods can be divided into two categories: pixel-based change detection and object-based change detection (OBCD) [4]. Pixel-based change detection detects the occurrence of changes based on direct comparison of pixels. It cannot overcome the limitations of radiometric differences and mis-registration between different dates [5]. Although object-based methods overcome this problem, they are difficult to determine a suitable segmentation scale for all kinds of objects in each temporal image. Over-segmentation and under-segmentation are not conducive to obtain better change detection results [6], [7].

Change detection can also be broadly categorized into unsupervised and supervised methods according to whether training samples are needed [8]. The former methods usually perform a direct binary segmentation with an unsupervised

algorithm. However, these results are influenced by the distribution of values in difference images and the characteristics of segmentation algorithms. Supervised methods can achieve better results with the prediction model learned by training samples. However, it is feasible only if training samples, which are not easy to be acquired, in research areas are obtained in advance.

Therefore, a novel change detection approach based on Morphological Profiles (MPs) and automated training sample extraction (ATSE) is proposed to overcome the problems in both unsupervised and supervised change detection methods. In this method, MPs are used to extract multi-scale structural features. ATSE is designed to extract the reliable changed and unchanged pixels from the initial results generated by unsupervised change detection method based on magnitude selection and Markov Random Field (MRF). Finally, the extracted MPs and refined training samples are put into the Support Vector Machine (SVM) to train and generate the final result.

## II. METHOD

The proposed approach, which is shown in Fig. 1, broadly includes the following steps: 1) Fundamental image pre-processing operations are conducted for bi-temporal remote sensing images, including radiometric correction, orthorectification, pan-sharpening and co-registration. 2) Change vector analysis (CVA) has been proven to be an effective change detection method [9]. In this research, change magnitude of each pixel is calculated. It represents the total gray-level difference between bi-temporal images. After that, Otsu algorithm is carried out to separate changed and unchanged regions from the change magnitude map [10]. Hence, the preliminary change detection map is generated. 3) MPs allow us to construct a comprehensive feature set, which is defined by a sequential filters of geodesic opening and closing with different sizes of the structuring element (SE) to model multi-scale structural information of an image [11]. With four-connected neighborhood considered, the marker and mask images represented the dilation and complement images of the input, which are the difference image in this research, are produced respectively. A disk shape of SE is selected and the sizes are increased from 1 to 5 to carry out a multi-scale

analysis using the reconstructed difference image generated at different scales [12]. 4) Although the change detection through CVA with spectral bands and Otsu algorithm can get a good result, some commission and omission errors are existed. Therefore, more reliable training samples are needed to be selected and combined with MPs to achieve a better result through a supervised process. For the training sample selection process, the following two steps are needed. The first step is selecting the pixels with the highest and lowest values in the change magnitude image (15 percent of highest and lowest values of change magnitude were selected in this research through trial and error). These pixels with the maximum and minimum cumulative variation considering all bands are most likely to be the changed and unchanged pixels. The second step is optimizing the initial change detection result by using MRF, which has shown to be effective in reducing the salt-and-pepper noise [13]. Therefore, MRF is carried out with the initial change detection map and difference image. After that, a modified change detection map with more homogeneous regions is achieved. Finally, the final training samples are obtained by intersecting the change and unchanged regions obtained by the aforementioned two steps. 5) Once the set of features and refined training samples to be involved in the change detection problem have been defined, SVM is adopted for supervised change detection step thanks to its intrinsic robustness to high dimensional datasets and to ill-posed problems [14]. In this study, the Gaussian radial basis function (RBF) is set as the kernel function and particle swarm optimization (PSO) is used to optimize the parameters for SVM [15].

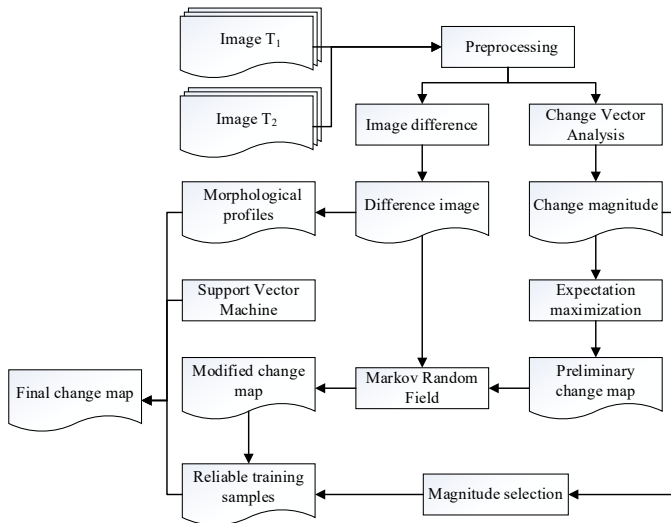


Fig. 1. Framework of the proposed change detection approach

### III. RESULTS AND ANALYSIS

#### A. Experiment A

The dataset of Experiment A, which was acquired from QuickBird satellite on 15 September 2004 and 2 May 2005, was located in Xuzhou City, China. After preprocessing, the

bi-temporal images were made up of  $1070 \times 1035$  pixels with spatial resolution of 0.61 m. The ground reference change map, which was used for testing the results, was produced through careful manual image-interpretation with prior knowledge and consisted of 121,101 unchanged pixels and 84,736 changed pixels, respectively. Fig. 2 depicted the true color composite images and reference change map of Experiment A. In the experiment, the proposed method were conducted with 100 training samples per class (totally 200) randomly selected from the training samples generated by ATSE. In order to proof the effectiveness of the proposed method, three methods: 1) change detection with EM algorithm and spectral bands (Spec-EM), 2) MRF after EM algorithm change detection (EM-MRF), 3) object-based change detection based on ATSE and SVM (OBCD-SVM), were implemented as comparisons. Note that ESP was conducted for OBCD-SVM to estimate more suitable scale parameter for multi-resolution image segmentation [16]. Table I listed the results of the change detection methods.

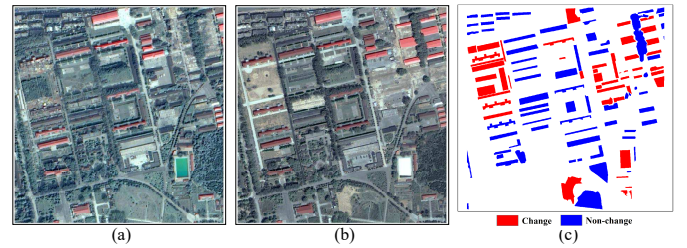


Fig. 2. True color composite images dataset acquired on (a) 15 September 2004 and (b) 2 May 2005, and (c) reference change map of Experiment A

TABLE I  
CHANGE DETECTION ACCURACIES OBTAINED BY THE PROPOSED APPROACH AND THE REFERENCE METHODS IN EXPERIMENT A

|        | Spec-EM | EM-MRF       | OBCD-SVM     | Proposed      |
|--------|---------|--------------|--------------|---------------|
| OA (%) | 81.35   | 84.51        | 83.73        | <b>86.37</b>  |
| Kappa  | 0.5977  | 0.6883       | 0.6509       | <b>0.7123</b> |
| UC (%) | 94.10   | 80.77        | <b>94.95</b> | 93.55         |
| CH (%) | 63.12   | <b>89.86</b> | 67.69        | 76.11         |
| CE (%) | 11.79   | 23.42        | <b>9.64</b>  | 10.81         |
| OE (%) | 36.88   | <b>10.14</b> | 32.31        | 23.89         |

UC: Unchanged class accuracy  
CE: Commission error

CH: Changed class accuracy  
OE: Omission error

From the table, it can be seen that the proposed method achieved better performances among the listing methods with the highest overall accuracy and Kappa coefficient. The results proof the effectiveness of the proposed approach in VHR image change detection. In more detail, EM-MRF had the best performance in detecting change regions and obtained the best changed class accuracy and omission error, while the OBCD-SVM had the best result in identifying unchanged areas and achieved the best result in unchanged class accuracy and commission error. Although these two methods achieved

the best performance in a certain type of detection, their overall accuracies were not as good as the proposed approach, which can take into account the accuracy of each class to get the highest overall accuracy. Fig. 3 showed the change detection map generated by different methods carried out in Experiment A. Compared with the other methods, the results generated by the proposed method can not only obtained less salt-and-pepper noise, but also effectively avoided some false and missed detection. Significant improvements achieved by using the proposed method were indicated with pairs of yellow rectangles in Fig. 3.

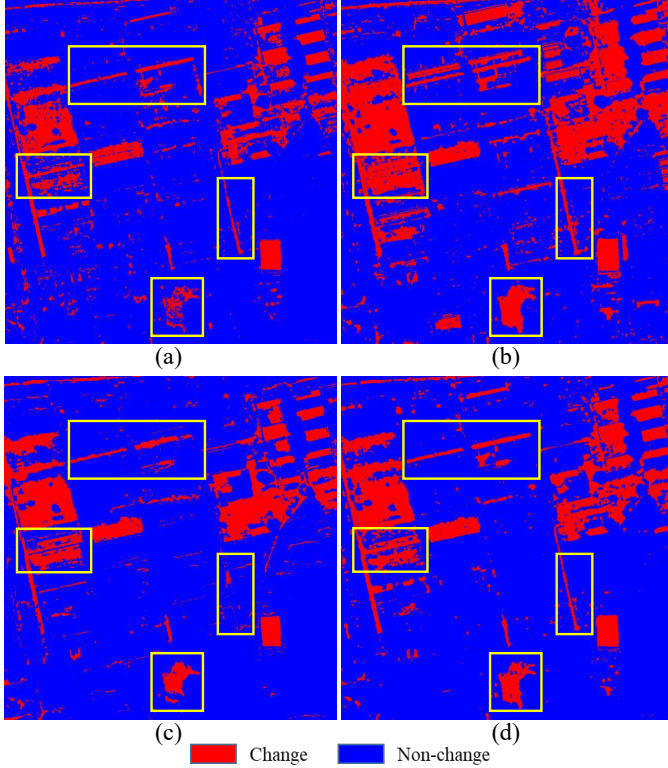


Fig. 3. Change detection map of (a) Spec-EM, (b) EM-MRF, (c) OBCD-SVM and (d) the proposed method in Experiment A

### B. Experiment B

The experimental area B were located in Jiangyin County, China. The images were obtained from Ziyuan-3 and Gaofen-1 satellites on 10 February 2015 and 27 March 2016. Although they were acquired from different sensors, they shared same multi-spectral bands with the same spectral range responses and were seen as the same source images in this research. After preprocessing, they were composed of  $800 \times 880$  pixels with spatial resolution of 2 m. In order to perform a quantitative analysis, the ground reference change map was produced through careful manual image-interpretation. Fig. 4 depicted the true color composite images and reference map, which consisted of 42,704 unchanged pixels and 24,586 changed pixels. In the experiment, 100 samples per class (totally 200) randomly selected from the training samples generated by ATSE were conducted to achieve the change detection result

in the proposed method. For the sake of demonstrating the superiority of this method, 1) Spec-EM, 2) EM-MRF, 3) OBCD-SVM were also implemented as comparisons. The change detection results of the aforementioned methods were listed in Table II.

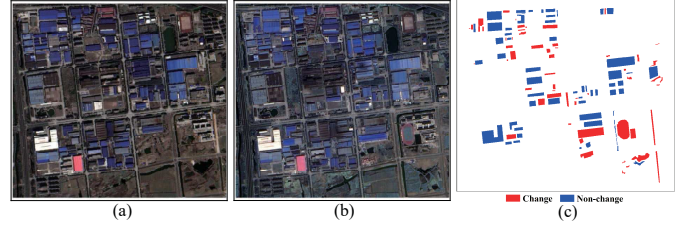


Fig. 4. True color composite images of dataset acquired on (a) 10 February 2015 and (b) 27 March 2016, and (c) reference change map of Experiment B

TABLE II  
CHANGE DETECTION ACCURACIES OBTAINED BY THE PROPOSED APPROACH AND THE REFERENCE METHODS IN EXPERIMENT B

|        | Spec-EM      | EM-MRF       | OBCD-SVM | Proposed      |
|--------|--------------|--------------|----------|---------------|
| OA (%) | 74.88        | 77.26        | 71.49    | <b>79.52</b>  |
| Kappa  | 0.4245       | 0.5469       | 0.3103   | <b>0.6322</b> |
| UC (%) | <b>88.21</b> | 70.91        | 85.87    | 86.74         |
| CH (%) | 51.73        | <b>88.28</b> | 43.03    | 76.40         |
| CE (%) | 28.36        | 36.40        | 36.32    | <b>23.16</b>  |
| OE (%) | 48.27        | <b>11.72</b> | 56.97    | 23.60         |

UC: Unchanged class accuracy  
CE: Commission error

CH: Changed class accuracy  
OE: Omission error

In Table II, with the comparison of the other methods, the proposed approach achieved the highest overall accuracy and Kappa coefficient. These results demonstrated that the proposed method outperformed the other methods and was more effective in unsupervised VHR remote sensing change detection. In the view of class specific accuracy, although Spec-EM and EM-MRF methods obtained better performances on changed class and unchanged class respectively, but they both had significant deficiencies on the other hand and the overall performances were not as good as the proposed approach. From the point of errors, the proposed method achieved the least commission error and the second least omission error, which means that it was provided with less errors in comparison with the other methods. The change detection map of each method was displayed on Fig. 5. It can be concluded from the figures that the proposed method effectively reduced some false and missed detections occurred in the other methods. The yellow rectangles in the figures highlighted some improvements of the proposed method.

### IV. CONCLUSIONS

A novel unsupervised change detection approach, which is based on a strategy of combining MPs and ATSE, is proposed in this paper. With multi-scale MPs, multi-level homogeneous structural features are extracted for modeling

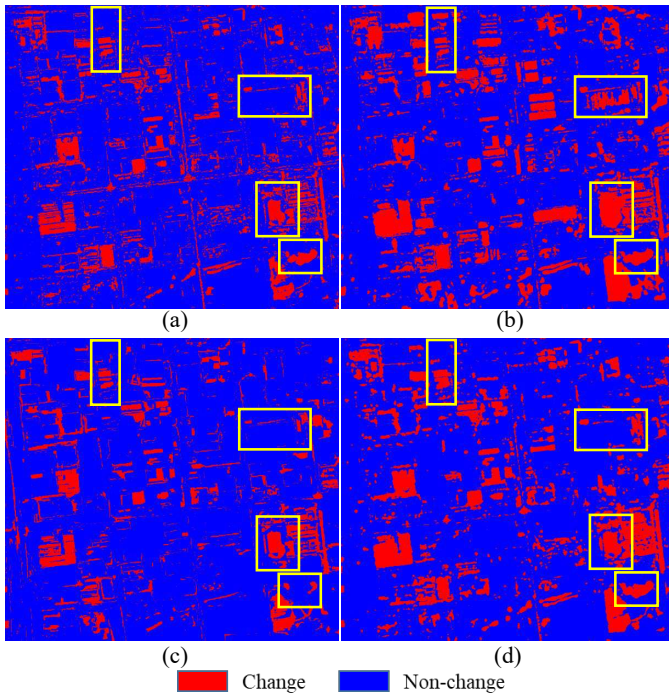


Fig. 5. Change detection map of (a) Spec-EM, (b) EM-MRF, (c) OB-CD-SVM and (d) the proposed method in Experiment B

change information of bi-temporal images. The ATSE method is proposed based on magnitude selection and CVA with MRF to refine more reliable training samples for the final change detection process. The experiments conducted with the real VHR datasets demonstrated that the proposed approach can effectively improve the overall change detection accuracy provided by state-of-the-art methods.

## REFERENCES

- [1] X.-P. Song, M. C. Hansen, S. V. Stehman, P. V. Potapov, A. Tyukavina, E. F. Vermote, and J. R. Townshend, "Global land change from 1982 to 2016," *Nature*, vol. 560, no. 7720, p. 639, 2018.
- [2] D. Lu, P. Mausel, E. Brondizio, and E. Moran, "Change detection techniques," *International Journal of Remote Sensing*, vol. 25, no. 12, pp. 2365–2401, 2004.
- [3] C. Marin, F. Bovolo, and L. Bruzzone, "Building change detection in multitemporal very high resolution sar images," *IEEE Transactions on Geoscience and Remote Sensing*, vol. 53, no. 5, pp. 2664–2682, 2015.
- [4] M. Hussain, D. Chen, A. Cheng, H. Wei, and D. Stanley, "Change detection from remotely sensed images: From pixel-based to object-based approaches," *ISPRS Journal of Photogrammetry and Remote Sensing*, vol. 80, pp. 91–106, 2013.
- [5] G. Chen, G. J. Hay, L. M. Carvalho, and M. A. Wulder, "Object-based change detection," *International Journal of Remote Sensing*, vol. 33, no. 14, pp. 4434–4457, 2012.
- [6] M. D. Hossain and D. Chen, "Segmentation for object-based image analysis (obia): A review of algorithms and challenges from remote sensing perspective," *ISPRS Journal of Photogrammetry and Remote Sensing*, vol. 150, pp. 115–134, 2019.
- [7] X. Wang, S. Liu, P. Du, H. Liang, J. Xia, and Y. Li, "Object-based change detection in urban areas from high spatial resolution images based on multiple features and ensemble learning," *Remote Sensing*, vol. 10, no. 2, p. 276, 2018.
- [8] S. Liu, D. Marinelli, L. Bruzzone, and F. Bovolo, "A review of change detection in multitemporal hyperspectral images: Current techniques, applications, and challenges," *IEEE Geoscience and Remote Sensing Magazine*, vol. 7, no. 2, pp. 140–158, 2019.
- [9] E. F. Lambin and A. H. Strahlers, "Change-vector analysis in multitemporal space: a tool to detect and categorize land-cover change processes using high temporal-resolution satellite data," *Remote Sensing of Environment*, vol. 48, no. 2, pp. 231–244, 1994.
- [10] N. Otsu, "A threshold selection method from gray-level histograms," *IEEE Transactions on Systems, Man, and Cybernetics*, vol. 9, no. 1, pp. 62–66, 1979.
- [11] M. Dalla Mura, J. A. Benediktsson, F. Bovolo, and L. Bruzzone, "An unsupervised technique based on morphological filters for change detection in very high resolution images," *IEEE Geoscience and Remote Sensing Letters*, vol. 5, no. 3, pp. 433–437, 2008.
- [12] S. Liu, Q. Du, X. Tong, A. Samat, L. Bruzzone, and F. Bovolo, "Multi-scale morphological compressed change vector analysis for unsupervised multiple change detection," *IEEE Journal of Selected Topics in Applied Earth Observations and Remote Sensing*, vol. 10, no. 9, pp. 4124–4137, 2017.
- [13] X. Chen, J. Chen, Y. Shi, and Y. Yamaguchi, "An automated approach for updating land cover maps based on integrated change detection and classification methods," *ISPRS Journal of Photogrammetry and Remote Sensing*, vol. 71, pp. 86–95, 2012.
- [14] G. Mountrakis, J. Im, and C. Ogole, "Support vector machines in remote sensing: A review," *ISPRS Journal of Photogrammetry and Remote Sensing*, vol. 66, no. 3, pp. 247–259, 2011.
- [15] S.-W. Lin, K.-C. Ying, S.-C. Chen, and Z.-J. Lee, "Particle swarm optimization for parameter determination and feature selection of support vector machines," *Expert Systems with Applications*, vol. 35, no. 4, pp. 1817–1824, 2008.
- [16] L. Druţ, D. Tiede, and S. R. Levick, "ESP: a tool to estimate scale parameter for multiresolution image segmentation of remotely sensed data," *International Journal of Geographical Information Science*, vol. 24, no. 6, pp. 859–871, 2010.